NANO LETTERS

LETTER

pubs.acs.org/NanoLett

Structural Transformation by Electrodeposition on Patterned Substrates (STEPS): A New Versatile Nanofabrication Method

Philseok Kim,[*,†,‡] Alexander K Epstein,[†,‡] Mughees Khan,[‡] Lauren D. Zarzar,[‡,§] Darren J. Lipomi,[§] George M. Whitesides,[‡,§] and Joanna Aizenberg[*,†,‡,§]

[†]School of Engineering and Applied Sciences, [‡]Wyss Institute for Biologically Inspired Engineering, [§]Department of Chemistry and Chemical Biology, Harvard University, Cambridge, Massachussets 02138, United States

Supporting Information

ABSTRACT: Arrays of high-aspect-ratio (HAR) nano- and microstructures are of great interest for designing surfaces for applications in optics, bio−nano interfaces, microelectromechanical systems, and microfluidics, but the difficulty of systematically and conveniently varying the geometries of these structures significantly limits their design and optimization for a specific function. This paper demonstrates a low-cost, high-throughput benchtop method that enables a HAR array to be reshaped with nanoscale precision by electrodeposition of conductive polymers. The method—named STEPS (structural transformation by electrodeposition on patterned substrates)—makes it possible to create patterns with proportionally increasing size of original features, to convert isolated HAR features into a closed-cell substrate with a continuous HAR wall, and to transform a simple parent two-dimensional HAR array into new three-dimensional patterned structures with tapered, tilted, anisotropic, or overhanging geometries by controlling the deposition conditions. We demonstrate the fabrication of substrates with continuous or discrete gradients of nanostructure features, as well as libraries of various patterns, starting from a single master structure. By providing exemplary applications in plasmonics, bacterial patterning, and formation of mechanically reinforced structures, we show that STEPS enables a wide range of studies of the effect of substrate topography on surface properties leading to optimization of the structures for a specific application. This research identifies solution-based deposition of conductive polymers as a new tool in nanofabrication and allows access to 3D architectures that were previously difficult to fabricate.

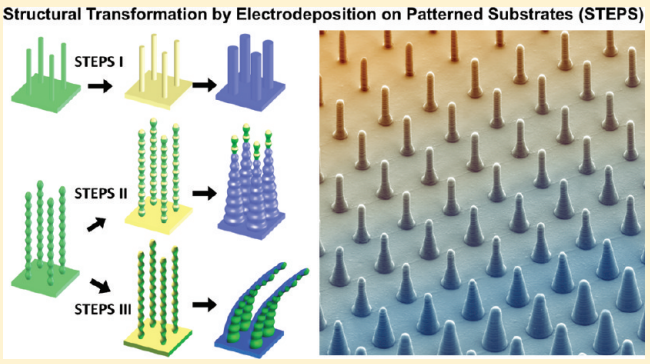

KEYWORDS: Nanofabrication, high-aspect-ratio nanostructure, electrodeposition, replica molding, gradient structure, three-dimensional patterning

Biomimetic architectures composed of arrays of high-aspect-ratio (HAR) micro/nanostructures have emerged as a new platform for applications in optics, surface science, and medicine. This class of structures (defined as structures with a ratio of height to width of >5) has been extensively studied as catalyst supports, scaffolds for tissue engineering, substrates for prevention of ice nucleation, biomimetic hybrid actuators, plasmonic structures, and microelectromechanical systems (MEMS) and for the control of adhesion, wetting, self-assembly, and heat transfer.[1−9] Typically, fabrication of arrays of HAR structures with long-range order requires a silicon master produced by expensive and laborious top-down lithography (e.g., optical or electron-beam lithography) and chemical or deep reactive ion etching (Bosch process).[10] Preparation of molds made of poly(dimethylsiloxane) (PDMS) or other elastomers with the negative structure of such silicon masters, and subsequent replication of the structure using different materials, allow multiple copies of the HAR structures to be produced with minimal damage to the original master.[11,12] Nevertheless, the size and shape of these HAR replicas are generally restricted to those of the parent structures. A new silicon master must thus be fabricated whenever a new structure is needed; this requirement for repeated fabrication of silicon masters significantly limits the ability to develop technologies using HARs.

Several approaches to fabricating arrays of structures with geometries different from those of the original silicon masters have been reported.[12−17] The intermediate elastomeric molds provide some freedom to modify the parent array by stretching, bending, shearing, and twisting the mold during the replication process.[12,13] The elastic instability of swelled PDMS membrane has been used to create a rich library of new patterns from a single master.[16] The solvent-assisted swelling of PDMS, in combination with heat-shrinkable and stretchable thermoplastic sheets, allows the alteration of the pattern density and symmetry of the master pattern, as well as limited reduction in size of molded features.[14] In most cases, however, these approaches are difficult to apply to

Received: February 4, 2011
Revised: March 16, 2011
Published: March 25, 2011

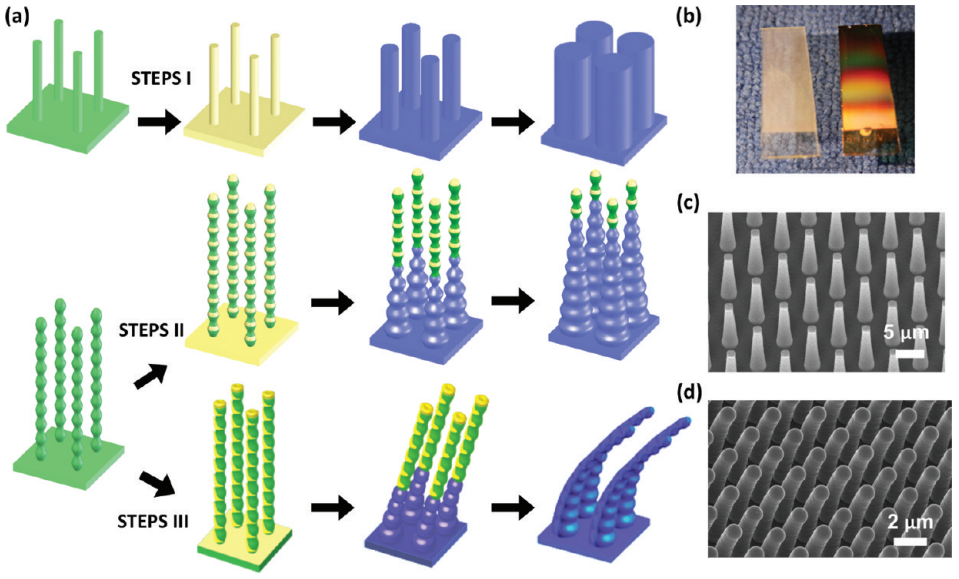

Figure 1. (a) Schematics showing the step-by-step structural transformation using sputter coated metal electrode (STEPS I), evaporated metal electrodes from the top (STEPS II), and evaporated metal electrodes at an angle (STEPS III): green, parent substrate; yellow, metal coating; blue, polypyrrole. (b) Photographs of a parent high-aspect-ratio nanopillar array (left) and a gradient nanopillar array modified by PPy deposition (right). (c) SEM image of an array of conical structures transformed from the original cylindrical nanopillar array produced using STEPS II process. (d) SEM image of an array of unidirectionally bent conical structures transformed from the original cylindrical nanopillar array using STEPS III process.

HAR structures, restricted to proportional modification of the original geometry, or limited by loss in fidelity of the patterns. No method is available for creating structures with modified 3D shape or gradient patterns of the sort that are particularly useful when conducting systematic studies of relations between structure and properties, and when examining multiple geometric parameters and their effects on surface properties (mechanical, electrical, adhesive, chemical, thermal, biocompatibility, etc.) using combinatorial screens.

Here we report a high-precision, high-throughput, and cost-effective benchtop nanofabrication method, in which a HAR pattern ("parent structure") can be reshaped with nanometer-scale precision by the deposition of conductive polymers. This method, which we call structural transformation by electrodeposition on patterned substrates (STEPS), makes it easy to proportionally change the size of the HAR nano/microstructures and produce three-dimensionally transformed tapered, anisotropic, and overhanging shapes, with the capability to create either continuous or stepwise gradient patterns from a single master structure. We demonstrate selected exemplary applications, including plasmonic nanostructure arrays, substrates for bacterial patterning, and the fabrication of mechanically reinforced structures.

Langer et al. and Melinte et al. have proposed that deposition of conductive polymers could be used as an element in nanofabrication.[18,19] For example, the fabrication of 3D microstructures, in which horizontally distributed arrays of patterned metal microelectrodes were sequentially connected electrically by the electrodeposited polypyrrole (PPy) film, has been reported.[18] Electroless deposition of polyaniline on platinum nanoelectrodes patterned by electron beam lithography (EBL) generated highly ordered 3D nanostructures of polyaniline.[19] Electrodeposition of PPy and similar redox-active conductive polymers (e.g., polyaniline, polythiophene) has been widely used due to its simplicity and low cost. These polymers are typically polymerized under oxidative (anodic) conditions; electrochemical polymerization eliminates the use of initiators. We deposited sodium dodecylbenzenesulfonate (NaDBS)-doped PPy on metallized arrays of HAR structures as proof-of-principle for the STEPS process, but the method can be extended to other conductive materials, given the solution used in the electrochemical deposition continues to wet the metallized arrays of HAR structures (i.e., maintains Wenzel state[20,21]) and to yield a smooth and uniform coating layer with a controllable rate of deposition.

As the starting substrate for electrodeposition, a commercial UV-curable epoxy resin (UVO114, Epotek) was cast in a PDMS mold bearing the negative of a parent structure to produce positive replicas.[12] The original Si master was fabricated by the Bosch process, and the HAR nanostructures therefore exhibited a characteristic wavy sidewall ("scalloping") that was precisely reproduced in the epoxy replica. A 30−100 nm thick gold or platinum layer was then deposited on this epoxy parent structure by either sputter coating or electron beam evaporation. The metal layer served as the working electrode in an electrochemical cell having a typical three-electrode configuration; PPy was electrochemically deposited from an aqueous solution containing 0.1 M pyrrole (Py) and 0.1 M NaDBS under a potentiostatic condition (0.5−0.7 V vs Ag/AgCl reference electrode). PPy deposition was also performed on a flat substrate to monitor the film thickness and the surface roughness. The rate of PPy deposition can be controlled by changing the voltage of electrodeposition, and can be maintained constant over at least a period of 20 min (See Figure S1, Supporting Information); precise control of voltage enables corresponding control of the size and shape of the resultant HAR structures.

Figure 1a summarizes the three schemes using STEPS combined with different methods of metallization (e.g., sputtering or evaporation). In scheme I, a continuous electrode was formed on the parent substrate by sputtering. In schemes II and III, a set of

dx.doi.org/10.1021/nl200426g |*Nano Lett.* 2012, 12, 527–533

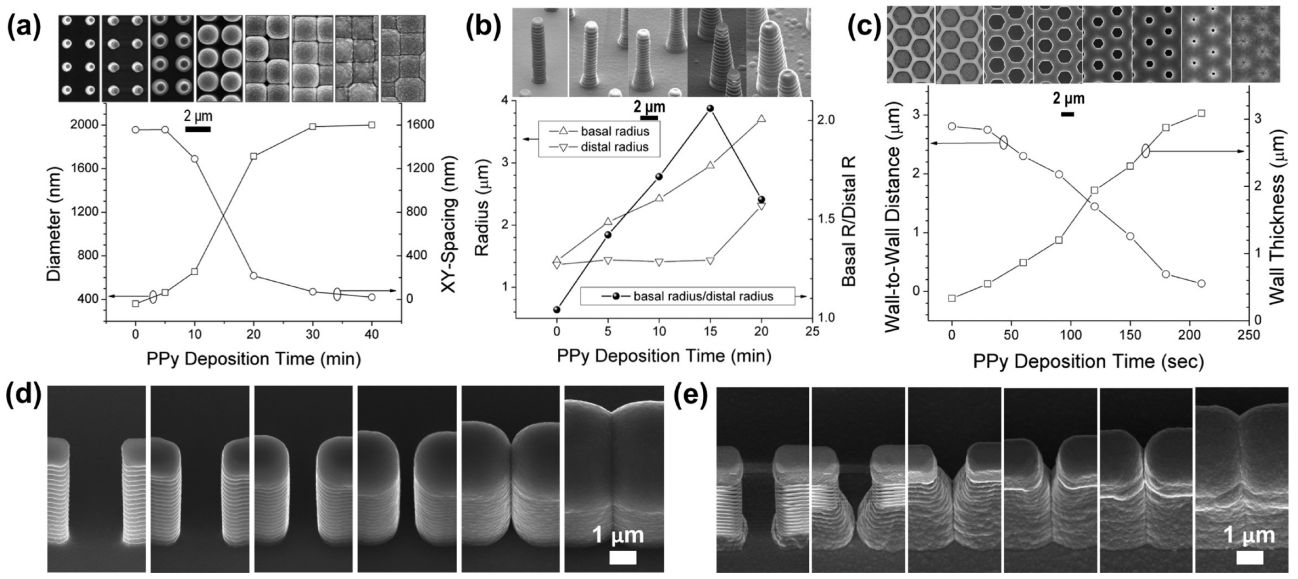

Figure 2. SEM images showing the modification of a parent structure using various STEPS methods. All the images are taken from epoxy replicas of the transformed structures. (a) Uniform structural transformation of a nanopillar array using sputter-coated metal electrode (STEPS I method). The plot shows the gradually increasing diameter of the pillars and the decreasing space between adjacent pillars as a function of the deposition time. (b) Transformation of a straight micropillar array into a tapered, conical micropillar array by using evaporated electrodes (STEPS II method). The plot shows the basal and distal radius and gradual increase in the ratio between the basal and distal radii of the structures as a function of the deposition time. (c) An interconnected array (honeycomb) undergoing uniform decrease in the size of honeycomb wells and increase in the wall thickness. (d, e) Comparison of the gap filling modes on the same parent substrate using sputter-coated metal electrode (d) and evaporated metal electrode (e). Electrodeposition was performed in an aqueous solution containing 0.1 M NaDBS and 0.1 M pyrrole. The deposition voltages are 0.55 V for (a) and (b) and 0.65 V for (c), (d), and (e).

discontinuous electrodes was formed by evaporation; the patterns here reflected shadowing due to scalloping of the sidewalls (scheme II) or due to a combination of scalloping and angled evaporation (scheme III). Electrodeposition of PPy on these metallized parent substrates would progressively transform the original structure into new geometries as illustrated schematically in Figure 1a. Electrodeposition of PPy on sputter-coated electrodes results in deposition of a smooth, uniform, and continuous film of PPy on the surface of the parent structures; this deposition transforms individual HAR structures into scaled replicas whose thickness has been changed conformally with time (Figure 1a, STEPS I). This process gradually increases the diameter of each micro/nanopillar, decreases the spacing between the adjacent pillars, and thus increases the space-filling factor of the substrate, as shown in Figure 2a for an exemplary HAR structure bearing a square array of nanopillars (distal diameter, 250 nm; basal diameter, 300 nm; height, 8 μm; pitch, 2 μm). As the gaps between adjacent nanopillar/PPy structures become narrower along the two lattice axes ([0, ±1] or [±1,0] directions), the diffusion of reactants from the solution into the small gaps becomes increasingly limited, while the diffusion around the gaps along the diagonals ([±1, ±1] directions) remains relatively unaffected. The rate of growth of PPy therefore becomes anisotropic, and the wider diagonal gaps are rapidly narrowed. As a result, the microstructures eventually fuse, and an array of diamond-shaped nanowells with a uniform, tunable size forms in the late stages of the deposition process (Figure 2a and Figure S2 in Supporting Information). Further replication of the nanowell structures provides an array of pillars with diamond-shaped cross sections, originating from cylindrically shaped columns. The STEPS I process therefore offers a sensitive tool that controls the size of features with nanometer resolution and, to a certain degree, the shape of the features in the horizontal, *XY* plane. It can also convert isolated structures into an interconnected wall or network.

Even more interesting is the unique ability of the STEPS process to modify the shape and size of the parent HAR structures in the *Z* direction and thus to lead to 3D modification of the nanostructures. Such modification can be achieved when parent structures have corrugated walls. Vertical *evaporative* metal deposition would then lead to shadowing and the formation of a set of isolated electrodes. PPy growth on these substrates would occur in a stepwise manner and generate structural transformations of the kind shown schematically in Figure 1a, STEPS II. As an example, we used an array of HAR nanopillars produced by the Bosch process that show pronounced scalloping of the sidewalls. The high directionality of the evaporated metal flume oriented normal to the sample prevents the metal from depositing on the shadowed areas on the underside of each scallop and yields a large continuous electrode on the substrate surface and a set of vertically isolated, distinct metal rings on each scallop. Electrodeposition of PPy using the electrode on the substrate surface as the working electrode initially results in the deposition of PPy on the substrate only, with no material deposition on the pillars. The deposited layer eventually connects electrically to the ring electrode on the first scallop when the PPy layer becomes thick enough to bridge the shadow-generated gap. Continuing the electrodeposition of PPy successively bridges vertically separated ring electrodes upward from the substrate. This procedure creates an effective gradient in the net electrodeposition time along the vertical axis of each HAR structure and causes the formation of highly uniform arrays of nano/microcones (Figure 1c) with increasing basal diameter that can be finely tuned by varying the deposition time (Figure 2b and Figure S3 in Supporting Information). The distal diameter of the

dx.doi.org/10.1021/nl200426g |*Nano Lett.* 2012, 12, 527–533

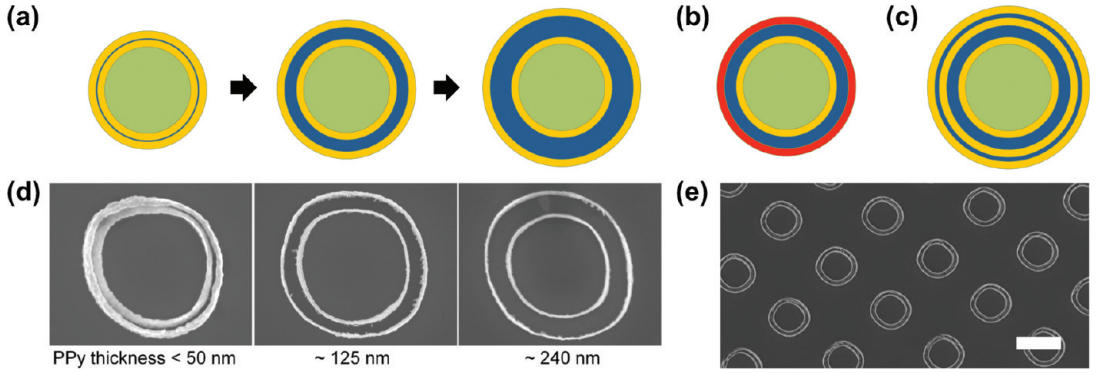

Figure 3. (a) Schematics of forming a gradient of concentric gold ring array with controlled gap size using gradient STEPS I method: green, core epoxy parent structure; yellow, sputter coated gold; blue, PPy. (b, c) Schematics of a concentric double ring structure with two different materials (b) and a concentric triple ring structure (c). (d, e) SEM images showing the gradually increasing gap between the inner and outer gold rings (d) and a region taken from a substrate with a gradient of concentric double rings (e). All of the sections were produced from a single substrate prepared using the gradient STEPS method. Scale bar = 2 μm.

features remains unchanged until the deposited layer reaches the electrode on the top surface of the pillars, gradually increasing the ratio between the sizes of the basal and distal ends of the pillars. Further deposition occurs in the manner described in the STEPS I process, where the cones thicken conformally at both the basal and the distal ends; uniform deposition results in scaled replicas with gradually decreasing basal-to-distal ratios. Panels d and e of Figure 2 visualize further the difference between the STEPS I and STEPS II processes by showing the evolution of the vertical cross sections of the same microstructures, where the gap between adjacent HAR pillars is filled by conformal "side-to-side" deposition of PPy that leaves the walls vertical in the case of sputtered metal electrode, while the gap is filled by "bottom-to-top" deposition of PPy onto evaporated metal electrodes.

New *anisotropic* geometries become possible when the metal electrodes are deposited onto the pillars at an angle from the evaporation source (for example, forming split-ring electrodes on each scallop) (Figure 1a, STEPS III process, and Figure S4 in Supporting Information). Electrodeposition on this substrate predominantly forms PPy on one side of the parent HAR structure and changes the mechanical properties of the structures anisotropically. Nanopillar arrays modified by this method tend to become unidirectionally bent and to have increased basal diameter as shown in Figure 1d; these types of structures can provide substrates with direction-dependent surface properties such as anisotropic wetting, adhesion, or friction.[22,23] Even more complex 3D microstructures can be fabricated by combining multiple STEPS methods, for example, by starting with a STEPS-modified structure or its replica, evaporating a new set of metal electrodes, and performing subsequent STEPS procedures.

High-aspect-ratio structures with interconnected walls (e.g., array of honeycomb wells or a brick wall) can also be modified by the STEPS process. For demonstration, an exemplary honeycomb structure was covered with conformally grown PPy when a sputter-coated electrode in STEPS I process was used; this type of electrodeposition continuously reduced the diameter of the wells from 3 μm to ~20 nm (Figure 2c). When a STEPS II process with evaporated electrodes was used, only the top surface of the closed cell walls was electrically connected and the electrodeposition takes place selectively on the top surface. This procedure effectively increases the depth of the well due to the material added on the top surface. Further deposition results in both vertical and lateral growth of the polymer layer at the distal end of the wall and bridging of the isolated electrodes downward; these processes combine to form slightly overhanging structures with the dimensions at the distal end larger than those at the basal end (Figure S5 in Supporting Information). Such surfaces provide re-entrant curvature, which is known to be an important feature for oleophobicity and low wettability by impacting liquid droplets.[20,21]

Since the STEPS method is a solution-based deposition method, all of the schemes for structural modification can be easily implemented to create continuous or stepwise gradients of feature sizes and shapes on a single substrate. To realize such structures, we used either continuous or stepwise withdrawal of the parent substrate from the electrodeposition bath by connecting the substrate to a syringe pump.[24] This procedure effectively creates a gradient of electrodeposition time along the axis of the substrate withdrawal (Figure 1b). Multiple gradients (e.g., orthogonal or triaxial) can also be formed on a single substrate by rotating the axes of gradients and subjecting the substrate to two or more electrodeposition steps with a specified gradient in each run. With a gradient-STEPS method, a substrate with different nanostructures (e.g., 250 different patterned regions in 3 cm^2) having precisely controlled dimensions was prepared; these heterogeneously structured substrates can be useful in systematic combinatorial studies of the effect of substrate topography on various surface properties. Examples include studies of the behavior of cells and bacteria on patterned substrates, adhesion, wetting, thermal transport, mechanical properties, as well as the effect of size and shape of surface patterns on the crystallization of materials.[1,2,9]

To demonstrate the unique capabilities of the STEPS method, we utilized it in a number of potential applications. We combined the STEPS method with nanoskiving—a nanofabrication method, in which sectioning with a microtome cuts thin slices from a block of composite material with embedded topographical patterns and generates multiple copies of indistinguishable nanostructures[25]—to produce sophisticated structures for optical applications, such as highly ordered periodic arrays of metallic concentric rings (ring resonators).[4] Figure 3 summarizes the procedure used for the fabrication of ordered arrays of plasmonic nanostructures comprising concentric gold nanorings. Briefly, an array of HAR epoxy nanopillars was coated by successive deposition: a first sputtered gold layer formed inner

dx.doi.org/10.1021/nl200426g |*Nano Lett.* 2012, 12, 527–533

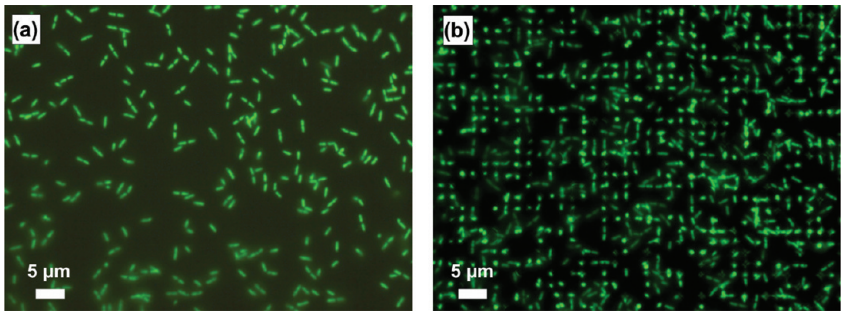

Figure 4. Fluorescence microscopy images of spontaneous bacterial patterning on an epoxy replica of a HAR nanopillar array modified by gradient-STEPS. A sputter coated electrode and a gradient of conformal PPy deposition were used to fabricate a gradient of nanopillar diameters, continuously varying the interstitial space available for biologically driven bacterial insertion. (a) No bacterial patterning on unmodified nanopillar array with wide interpillar spacings relative to bacteria scale. (b) Robust patterning occurs on widened pillars as the interstitial space decreases.

rings, electrodeposition of a second layer of PPy film formed a spacer layer, and a second sputtering formed an additional gold layer. This four-layered structure was embedded in epoxy and subjected to cutting by the ultramicrotome to generate thin, sliced sections containing periodic arrays of metallic concentric nanorings with a PPy spacer layer. The sections were collected and transferred to a substrate, and the PPy spacer layer and the parent epoxy core were selectively removed by oxygen plasma treatment (Figure 3d). The gap between the two gold nanorings was quickly optimized by a single gradient STEPS run. Such large-area nanoscale concentric metallic ring arrays with precisely controlled inter-ring spacing are quite challenging to fabricate, either by existing lithographic techniques or by elementary applications of nanoskiving (Figure 3e). Periodic arrays of concentric gold rings have double localized surface plasmon resonances and exhibit a large local field enhancement potentially useful for SERS sensors.[4,26] Fabrication of more complex optical structures at nanometer scales (such as, for example, multiring arrays or rings made of different metals, as shown in Figure 3b,c) is made possible by using the STEPS method, and the characterization of their optical properties is underway.

Figure 4 shows the application of STEPS to study the spontaneous patterning of rod-shaped bacteria on a nanostructured surface. We have shown earlier that a range of bacterial species display an affinity for surface attachment and evidently seek to maximize their contact area with the surface; the attachment leads to distinct patterns when periodic topography is present.[2] To examine this phenomenon further, and to prove the hypothesis that the bacteria indeed tend to maximize their surface contact, a range of structures with variable pitch, post diameter, and gap width is required. We applied the gradient-STEPS method with a sputtered metal electrode and continuous withdrawal to create 2D-gradient substrates, in which a gradient of the pitch between uniformly sized pillars in one direction was coupled with a gradient of the pillar diameters in the orthogonal direction. This combination of methods creates a gradient of interstitial spacing and pillar diameters across a centimeter-scale sample. Fluorescence imaging demonstrated spontaneous patterning of bacteria grown on the gradient array. This approach enables precise determination of the substrate geometry and feature sizes that induce specific bacterial responses. For example, Figure 4 shows that as the spacing between the posts decreases, the order of the bacterial pattern increases significantly. Indeed, both the pitch and wall-to-wall spacing of surface nanostructures can be adjusted by combining pitch-gradient Si master fabrication with gradient-STEPS method to probe this phenomenon, and a systematic study of bacterial behavior on tailored double-gradient substrates will be published elsewhere.

While HAR nanopillars were shown to be widely useful for photonic, electronic, energy, and fluidics applications, their poor mechanical stability results in breaking and collapse, and makes them vulnerable and often nonpractical in real technologies. The STEPS process provides a simple means to create mechanically reinforced nanostructures through either uniform conformal coating of these structures using the STEPS I process or controlled increase of their basal size. Figure 5 shows the mechanical reinforcement of a microstructured array by shape transformation using STEPS methods. The arrays of Y-shaped microposts in these SEM images were strengthened by either uniformly increased thickness following conformal PPy deposition, STEPS I (Figure 5a), or by increased base thickness following STEPS II (Figure 5b). In the latter case, the structures become tapered in cross section and have increased width at the bottom to resist bending stresses. We used an Agilent G200 nanoindentation system to compare the structural deformation of the original Y-micropost structure (Figure 5c, left) and incrementally reinforced microstructures. The cell-centered 10 mN nanoindentations were applied with a standard Berkovich tip. Figure 5c shows that permanent deformation sharply decreased as the structure was reinforced. Figure 5d shows finite element method (FEM) simulations to model the structural response of the epoxy replicas of the original Y-micropost and a STEPS-reinforced Y-micropost. A 5-μm-tall original Y-micropost structure with arm length of 4 μm and a width of 1 μm was modeled using COMSOL FEM software. The tapered Y-micropost structure was 2 μm wide at the bottom and tapered to 1 μm at the top. We assumed a uniformly distributed compressive load of 100 MPa for both structures, using the material properties of UV-cured epoxy resin. The tapered micropost structure shows a 2-fold decrease in the maximum induced stresses compared to that of the original Y-micropost. The array of Y-shaped microposts was specifically used here to demonstrate the range of characteristic features of the shape evolution in the STEPS process. Among other properties, it provides a good example of the transformation of isolated columns into a closed-cell structure with interconnected walls.

In conclusion, we have developed a new nanofabrication method, STEPS (structural transformation by electrodeposition on patterned substrates), which offers rapid fabrication of high-aspect-ratio nanostructures with feature sizes tunable in the

dx.doi.org/10.1021/nl200426g |*Nano Lett.* 2012, 12, 527–533

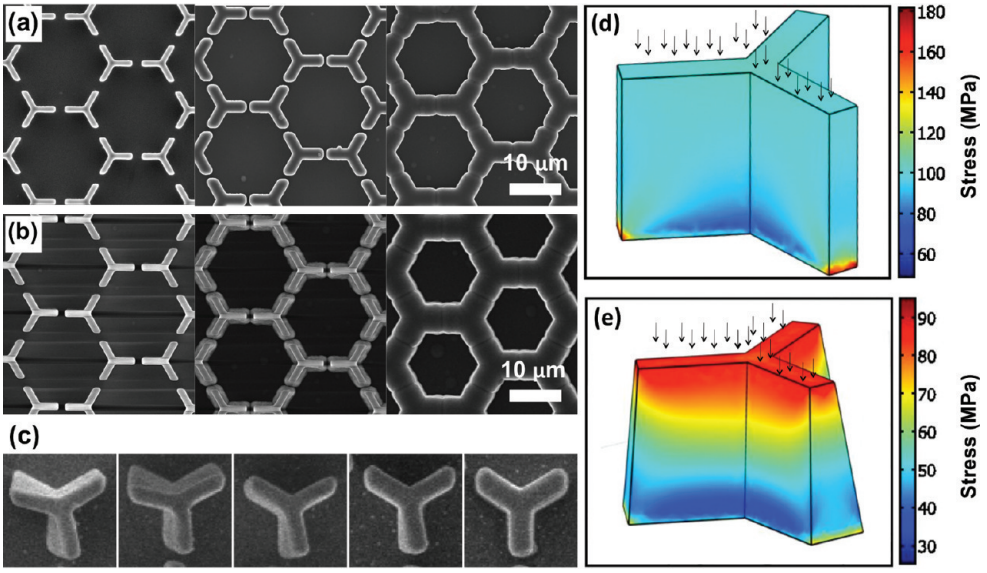

Figure 5. SEM images showing mechanical reinforcement of a microstructure by shape transformation using STEPS methods. All the images are of epoxy replicas of STEPS-modified structures. (a) Increasing the thickness of the structure using sputter-coated metal electrodes. (b) Formation of a tapered cross section using evaporated metal electrodes. (c) Comparison of the mechanical stability of epoxy replicas of the original structure (left) and incrementally reinforced microstructures (from left to right) following a series of cell-centered 10 mN nanoindentations with a Berkovich tip. (d, e) FEM simulations for an original microstructure (d) and a STEPS-modified, tapered microstructure (e) under a distributed compression loading of 100 MPa. Height = 5 μm, arm = 4 μm, width = 1 μm. STEPS-reinforced tapered structure shows a 2-fold decrease in the maximum induced stress compared to the original structure.

nanometer range with high fidelity. This method transforms the original features of vertical HAR geometries and generates a range of 3D shapes—including tapered or overhanging structures—with the capability to create either uniform features over a large area or gradient patterns (continuous or discrete) from a single master. Such substrates are very challenging to fabricate using conventional techniques. All of these new patterns can serve as new masters for replication provided there is no pronounced reentrant curvature. Furthermore, subsequent deposition of other materials (e.g., noble metals or semiconductors) on the 3D-patterned conductive polymer surface would lead to new applications. We believe that the STEPS method will be useful in the research that utilizes arrays of HAR nano/microstructures by offering many research laboratories the ability to create new patterns (including gradient substrates) inexpensively and conveniently. We are currently using combinatorial STEPS substrates in many ongoing studies (to be published subsequently).

■ ASSOCIATED CONTENT

Ⓢ Supporting Information. Experimental details, PPy deposition rate, surface roughness of deposited PPy layer, SEM images of various STEPS-produced nanostructures described in the main text but not displayed in the main text. This material is available free of charge via the Internet at http://pubs.acs.org.

■ AUTHOR INFORMATION

Corresponding Author

*E-mail: jaiz@seas.harvard.edu or pkim@seas.harvard.edu.

■ ACKNOWLEDGMENT

Research supported by the U.S. Department of Energy, Office of Basic Energy Sciences, Division of Materials Sciences and Engineering under Award #DE-SC0005247 (fabrication of HAR structures) and by the U.S. Army Research Office Multidisciplinary University Research Initiative under Award #W911NF-09-1-0476 (reinforced structures). We thank Professor Theodore Betley for the use of equipment, Dr. Alison Grinthal for helpful comments, and Dr. James C. Weaver for graphic artwork. This work was carried out in part through the use of MIT's Microsystems Technology Laboratories and Harvard's Center for Nanoscale Systems (CNS).

■ REFERENCES

(1) Bettinger, C. J.; Langer, R.; Borenstein, J. T. *Angew. Chem., Int. Ed.* **2009**, *48*, 5406–5415.
(2) Hochbaum, A. I.; Aizenberg, J. *Nano Lett.* **2010**, *10* (9), 3717–3721.
(3) Kim, P.; Zarzar, L. D.; Zhao, X.; Sidorenko, A.; Aizenberg, J. *Soft Matter* **2010**, *6* (4), 750–755.
(4) Lipomi, D. J.; Kats, M. A.; Kim, P.; Kang, S. H.; Aizenberg, J.; Capasso, F.; Whitesides, G. M. *ACS Nano* **2010**, *4* (7), 4017–4026.
(5) Mishchenko, L.; Hatton, B.; Bahadur, V.; Taylor, J. A.; Krupenkin, T.; Aizenberg, J. *ACS Nano* **2010**, *4* (12), 7699–7707.
(6) Sidorenko, A.; Krupenkin, T.; Aizenberg, J. *J. Mater. Chem.* **2008**, *18*, 3841–3846.
(7) Sidorenko, A.; Krupenkin, T.; Taylor, A.; Fratzl, P.; Aizenberg, J. *Science* **2007**, *315*, 487–490.
(8) Pokroy, B.; Kang, S. H.; Mahadevan, L.; Aizenberg, J. *Science* **2009**, *323*, 237–240.
(9) Vasquez, Y.; Fenton, E. M.; Chernow, V. F.; Aizenberg, J. *Cryst. Eng. Commun.* **2011**, *13*, 1077–1080.
(10) McAuley, S. A.; Ashraf, H.; Atabo, L.; Chambers, A.; Hall, S.; Hopkins, J.; Nicholls, G. *J. Phys. D: Appl. Phys.* **2001**, *34*, 2769–2774.
(11) Zhang, Y.; Lo, C.-W.; Taylor, J. A.; Yang, S. *Langmuir* **2006**, *22*, 8595–8601.
(12) Pokroy, B.; Epstein, A. K.; Persson-Gulda, M. C. M.; Aizenberg, J. *Adv. Mater.* **2009**, *21*, 463–469.

(13) Xia, Y.; Whitesides, G. M. *Angew. Chem., Int. Ed.* **1998**, *37*, 550–575.
(14) Lee, M. H.; Huntington, M. D.; Zhou, W.; Yang, J.-C.; Odom, T. W. *Nano Lett.* **2011**, *11*, 311–315.
(15) Zhang, Y.; Lin, C.-T.; Yang, S. *Small* **2010**, *6* (6), 768–775.
(16) Zhang, Y.; Reed, J. C.; Yang, S. *ACS Nano* **2009**, *3* (8), 2412–2418.
(17) Xia, Y.; Rogers, J. A.; Paul, K. E.; Whitesides, G. M. *Chem. Rev.* **1999**, *99*, 1823–1848.
(18) LaVan, D. A.; George, P. M.; Langer, R. *Angew. Chem., Int. Ed.* **2003**, *42* (11), 1262–1265.
(19) Vlad, A.; Dutu, C. A.; Guillet, P.; Jedrasik, P.; Fustin, C.-A.; Södervall, U.; Gohy, J.-F.; Melinte, S. *Nano Lett.* **2009**, *9* (8), 2838–2843.
(20) Ahuja, A.; Taylor, J. A.; Lifton, V.; Sidorenko, A. A.; Salamon, T. R.; Lobaton, E. J.; Kolodner, P.; Krupenkin, T. N. *Langmuir* **2008**, *24*, 9–14.
(21) Tuteja, A.; Choi, W.; Ma, M.; Mabry, J. M.; Mazzella, S. A.; Rutledge, G. C.; McKinley, G. H.; Cohen, R. E. *Science* **2007**, *318*, 1618–1622.
(22) Kwak, M. K.; Jeong, H.-E.; Kim, T.-i.; Yoon, H.; Suh, K. Y. *Soft Matter* **2010**, *6*, 1849–1857.
(23) Chu, K.-H.; Xiao, R.; N.Wang, E. *Nat. Mater.* **2010**, *9*, 413–417.
(24) Withdrawal of the parent substrate from the electrodeposition solution works better than immersion of the substrate due to the wicking of the solution into the nanostructured surface.
(25) Xu, Q.; Rioux, R. M.; Dickey, M. D.; Whitesides, G. M. *Acc. Chem. Res.* **2008**, *41* (12), 1566–1577.
(26) Lipomi, D. J.; Martinez, R. V.; Kats, M. A.; Kang, S. H.; Kim, P.; Aizenberg, J.; Capasso, F.; Whitesides, G. M. *Nano Lett.* **2011**, *11*, 632–636.

NOTE ADDED AFTER ASAP PUBLICATION

The Acknowledgments were modified in the version of this paper published on March 25, 2011. The correct version published March 31, 2011.